Crystallization of Poly(ethylene terephthalate)/ Polycarbonate Blends. I. Unreinforced Systems

VERONIKA E. REINSCH and LUDWIG REBENFELD*

TRI/Princeton, and Department of Chemical Engineering, Princeton University, P.O. Box 625, Princeton, New Jersey 08542

SYNOPSIS

The crystallization and transition temperatures of poly(ethylene terephthalate) (PET) in blends with polycarbonate (PC) is considered using thermal analysis. Additives typically used in commercial polyester blends, transesterification inhibitor and antioxidant, are found to enhance the crystallization rate of PET. Differential scanning calorimetry (DSC) reveals two glass transition temperatures in PET/PC blends, consistent with an immiscible blend. Optical microscopy observations are also consistent with an immiscible blend. Small shifts observed in the T_g of each component may be due to interactions between the phases. The degree of crystallinity of PET in PET/PC blends is significantly depressed for high PC contents. Also, in blends with PC content greater than 60 wt %, two distinct crystallization exotherms are observed in dynamic crystallization from the melt. The isothermal crystallization kinetics of PET, PET modified with blend additives, and PET in PET/PC blends have been evaluated using DSC and the data analyzed using the Avrami model. The crystallization of PET in these systems is found to deviate from the Avrami prediction in the later stages of crystallization. Isothermal crystallization data are found to superimpose when plotted as a function of time divided by crystallization half-time. A weighted series Avrami model is found to describe the crystallization of PET and PET/PC blends during all stages of crystallization. © 1996 John Wiley & Sons, Inc.

INTRODUCTION

The crystallization of poly(ethylene terephthalate) (PET) in blends of PET and polycarbonate (PC) is of critical importance in the melt processing of such blends. This article deals with the effects of the amorphous PC phase and typical PET/PC blend additives on crystallization kinetics, morphology, and transition temperatures of PET. Part II of this series will consider the influence of reinforcing fibers on the crystallization of PET in PET/PC blend composites.

Much previous research in the area of PET/PC blends has focused on component miscibility. Based on the observation of only one T_g, one group reported that PET and PC are miscible for compositions containing at least 60 wt % PET.[1] On the other hand, for PC-rich compositions, where two T_g's were observed, it was proposed that two amorphous phases exist.[1] Other researchers reported that PET and PC are immiscible based on thermal analysis, infrared spectroscopy (IR), phase contrast microscopy, and dynamic mechanical analysis.[2-6] Yet another study suggested that these polymers are somewhat compatible; that is, the compatibility is higher in the PET rich phase than in the PC-rich phase.[7]

Some researchers suggest that the compatibility of PET and PC is dependent on the level of transesterification.[2,3] In the absence of transesterification, these polymers are incompatible.[8] Transesterification reactions have been studied by a number of researchers as a function of blend composition, residual catalyst, and melt processing time and temperature.[9-12] Complications resulting from transesterification reactions have led to the development of transesterification inhibitors. One study of organophosphites indicates that these compounds are effective in inhibiting transesterification in PET/PC blends with some residual moisture and ineffective in dried blends.[13]

* To whom correspondence should be addressed.

Journal of Applied Polymer Science, Vol. 59, 1913–1927 (1996)
 CCC 0021-8995/96/121913-15

The effect of blending on the crystallinity of PET has been investigated using differential scanning calorimetry (DSC) and IR. DSC results indicate that the crystallinity of PET decreases with increasing PC content, and that for blend compositions with 20 wt % PET and less, the crystallinity of PET is negligible.[14] However, this study was performed on blends which exhibited only one T_g and which had therefore likely undergone extensive transesterification. Chen and Birley[5] studied PET/PC blends using IR and DSC and showed that the crystallinity of PET in PC-rich samples is suppressed. Hanrahan et al.[15] report a constant degree of crystallinity in PET/PC for all blend compositions.

Chen and Birley[5] also report an effect of blending on the T_g of PC. The T_g of PC decreases from 147°C in 100% PC to 138°C in 60/40 PET/PC, while T_g of PET remains relatively constant. Similar results concerning component T_g's were reported by Hanrahan et al.[15] These authors also studied the melting behavior of PET in PET/PC and found that the melting temperature of PET decreases with decreasing PET content in the blend.

EXPERIMENTAL

Poly(ethylene terephthalate)/polycarbonate (PET/PC) blends were supplied by the General Electric Company in pellet form: 80/20 PET/PC (80 wt % PET/20 wt % PC), 60/40 PET/PC, 40/60 PET/PC, and 20/80 PET/PC. In addition, samples of 100% PET (Traytuf 7200C, M_n 16,000) and 100% PC (Lexan 141, M_w 57,000; M_n 24,000) were supplied. These are the same resins used in the preparation of the blends. Finally, because the blend samples contain a proprietary transesterification inhibitor and antioxidant, a sample was prepared of the same PET with transesterification inhibitor and antioxidant, so that the effect of these blend additives on PET crystallization could be determined and distinguished from the effects of the PC component. The antioxidant is Irganox 1076 (two parts per thousand loading), produced by Ciba-Geigy.

The blend samples were molded into films by placing approximately 15 g of resin pellets between two sheets of Teflon®-coated glass release fabric and molding on a hot press at 275°C for 1 min at a pressure of 200 psi. All films were dried for 16 h in a vacuum oven at 100°C. Films were then molded for a second time for 8 min in order to simulate the fabrication of fiber-reinforced composites.

Thin films were prepared for optical microscopy by placing five small pieces of film, totaling approximately 1 mg, on a glass coverslip. The coverslip was placed on the bottom platen of a hot press at 320°C, covered with another glass coverslip, and pressed with forceps to produce a thin film. The sample was crystallized dynamically for 1 min at approximately 100°C and then quenched for examination in an optical microscope under polarized light.

Specimen weights for differential scanning calorimetry (DSC), using a Perkin-Elmer DSC-4, varied from 4 to 20 mg, so the PET content in each specimen was roughly 4 mg. Samples were first scanned in the DSC from 25°C to 280°C at 10°C/min to determine the glass transition temperature, T_g, of each component. In cases where the recrystallization exotherm of PET overlapped with the T_g of PC, the sample was heated to 150°C, cooled at 320°C/min to 90°C, and scanned again at 10°C/min to 280°C.

In isothermal crystallization experiments, samples were scanned to 280°C, held for 5 min, and then quenched at 320°C/min to the crystallization temperature of interest. Crystallization temperatures in the range of 210 to 235°C were investigated. When heat flow no longer changed with time, the sample was cooled to 15°C below the crystallization temperature and then scanned at 10°C/min to 280°C to collect melting data. To avoid cumulative thermal history effects and degradation, a new specimen was used for each crystallization experiment. All crystallizations were repeated three times. Dynamic crystallization from the melt was also studied: Samples were scanned to 280°C, held for 5 min, and then cooled at 5°C/min to 25°C.

The effects of melt processing on crystallization behavior were examined for the 60/40 PET/PC blend. The samples were scanned to a chosen melt processing temperature, held for a given melt time, and then quenched to 220°C, where isothermal crystallization was observed. Melt processing temperatures were 280 and 300°C, and melt times were 1, 5, 10, 20, and 30 min. When crystallization was complete, fusion data for the crystallized sample were collected by scanning from 205°C to 280°C.

RESULTS AND DISCUSSION

Morphology of PET/PC Blends

Figure 1 shows a micrograph of 60/40 PET/PC suggesting two phases in this blend. The one phase is composed of crystalline material in which the morphology is spherulitic, exhibiting Maltese cross extinction patterns typical of PET.[16] The other

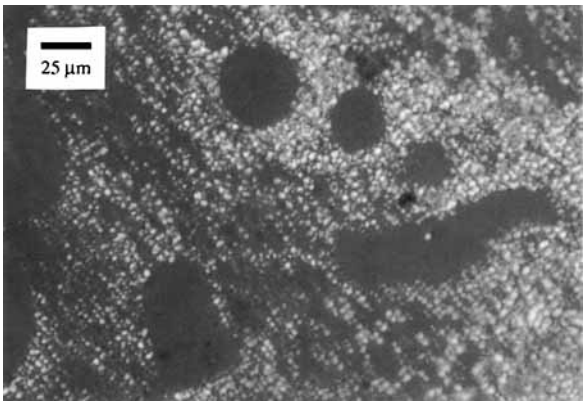

Figure 1 Optical micrograph of 60/40 PET/PC.

phase shows no signs of order and appears to be amorphous. The micrograph is consistent with the morphology of an immiscible blend of crystalline and amorphous polymers.

The sizes of the spherulitic domains in Figure 1 vary from approximately 10 μm in diameter to over 100 μm. It is possible that the size and shape of domains have been affected by the prior thermal and mechanical processing of the blend. The morphologies observed in the other blend compositions are similar to that shown in Figure 1, with the exception of the 20/80 PET/PC blend. In this blend, for the crystallization period allowed, no order is observed to develop.

Glass Transition in PET/PC Blends

Heating scans of quenched samples show either two glass transition temperatures for PET and PC or a single glass transition for PET and recrystallization of PET, which masks the glass transition of PC. In cases where the recrystallization of PET masks the T_g of PC, a second scan is performed after the recrystallization of PET is complete. Figure 2 shows a scan of 20/80 PET/PC, in which two T_gs are observed. Since the recrystallization exotherm for PET in this blend is very weak, the T_g of PC is not obscured. In Figure 3, only the T_g of PET, followed by recrystallization of PET, is observed for 60/40 PET/PC. On the same plot, a second scan, performed after recrystallization of PET is complete, shows the T_g of PC at 141°C.

The T_gs of PET and PC are summarized in Table I for the range of compositions studied. "Modified PET" refers to the PET sample with added transesterification inhibitor and antioxidant. The distinct T_gs observed indicate that these polymers are immiscible. It is interesting that the T_g of PET in the blends is slightly higher than that of 100% PET,

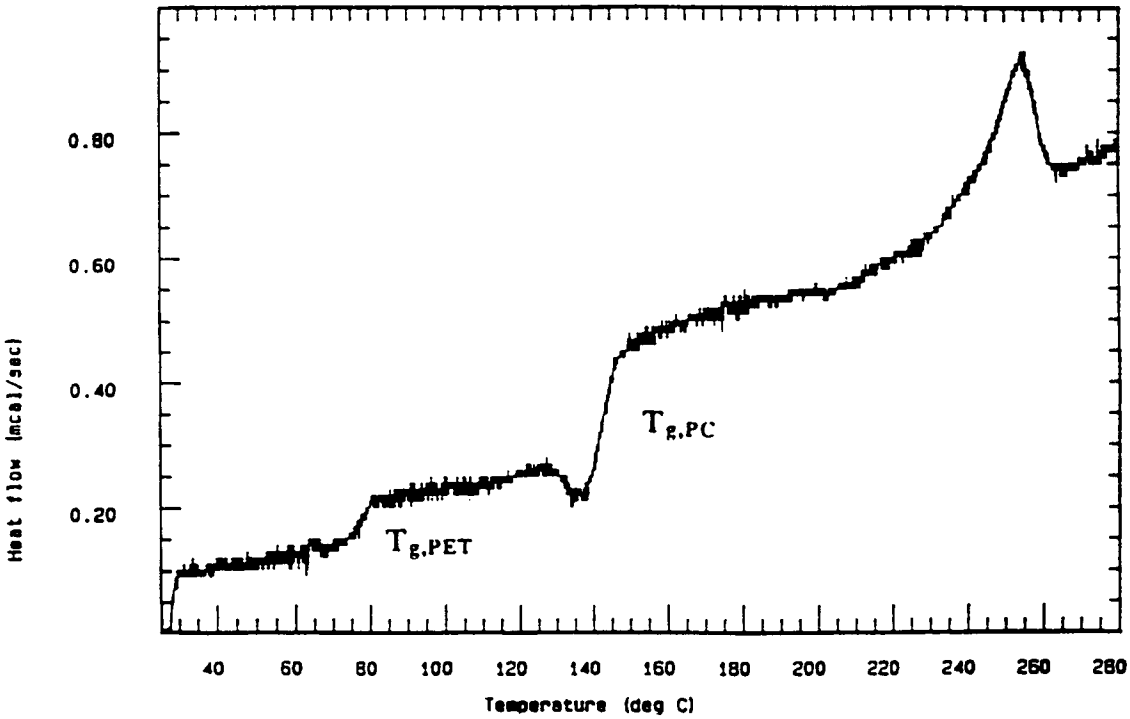

Figure 2 Scan of 20/80 PET/PC blend showing the glass transition temperatures of PET and PC.

while the T_g of PC is lower than that of 100% PC. The same shifts in component T_gs have previously been observed in PET/PC blends.[1] Since the glass transition of PET takes place in the presence of *glassy* PC, the rigid PC "matrix" could contribute toward increasing the T_g of PET. The presence of rigid domains may act to raise T_g through a friction or wall effect. It is noted, however, that the shift in PET T_g in the blends, while consistent in all samples, is not large and is only slightly greater than the uncertainty in the measurements. The depression in T_g of PC is somewhat greater in magnitude than the PET shift. The glass transition of PC in the blend takes place in the presence of *rubbery* PET, which may effectively plasticize the PC at the interface. This would explain the observed depression of PC T_g in the blends. Alternatively, it is possible that some transesterification has occurred in the blend samples during processing. This would cause some convergence in the T_g values through homogenization introduced by the newly created copolymer.

Table I Glass Transition Temperature of PET and PC in Blend Samples Determined by DSC Scans in Heating Mode with Scan Rate of 10°C/min

Sample	$T_{g,PET}$ (°C)	$T_{g,PC}$ (°C)
PET	75 ± 1	—
Modified PET	75 ± 1	—
80/20 PET/PC	77 ±1	140 ± 1
60/40 PET/PC	76 ± 1	141 ± 2
40/60 PET/PC	76 ± 1	140 ± 1
20/80 PET/PC	76 ± 2	143 ± 1
PC	—	145 ± 2

Recrystallization in PET/PC Blends

The recrystallization temperature is taken to be the maximum of the dynamic crystallization peak in a heating scan (e.g., Fig. 3), and the data are summarized in Table II. The recrystallization temperature is significantly lower for the modified PET-containing blend additives compared with PET, indicating a significant enhancement of the rate of cold crystallization. This rate enhancement may result from one or both of the additives enhancing chain mobility. Alternatively, it is possible that the additives affect the nucleation behavior of PET.

Recrystallization temperature in PET/PC blends passes through a minimum with composition. Thus,

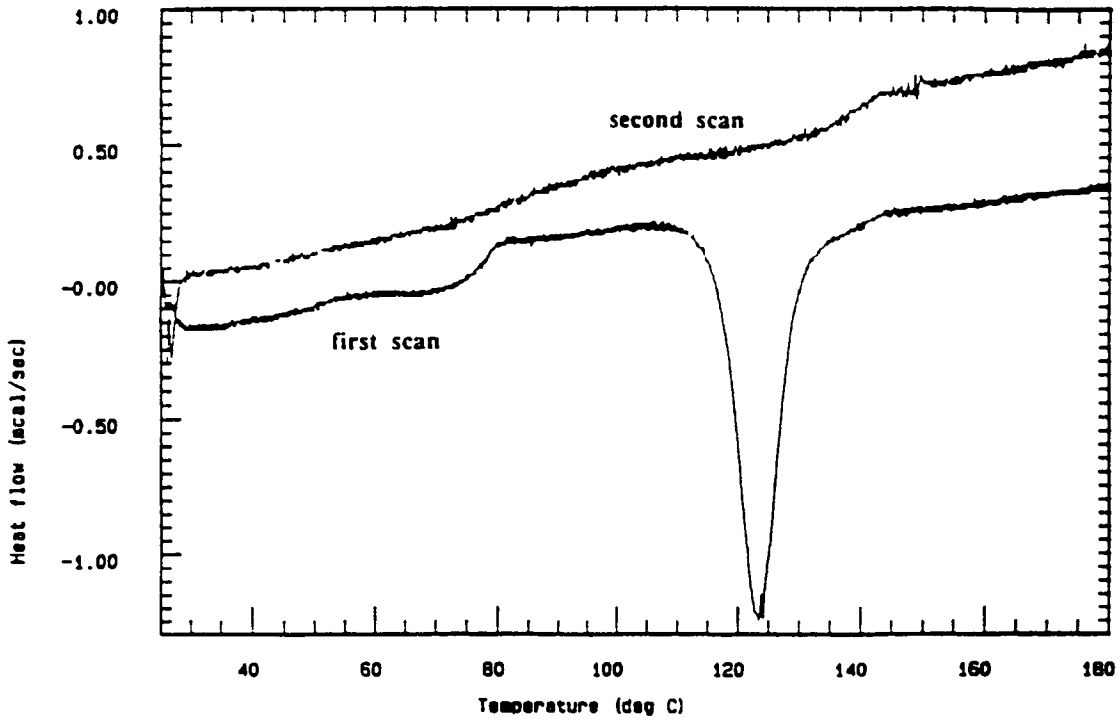

Figure 3 First scan of 60/40 PET/PC blend showing only the glass transition temperature of PET, and a second scan showing the glass transition temperature of PC.

Table II Recrystallization Temperature (°C) of PET in Blend Samples as Determined from DSC Heating Scans

Sample	Recrystallization Temperature (°C)
PET	138 ± 2
Modified PET	127 ± 2
80/20 PET/PC	124 ± 3
60/40 PET/PC	123 ± 4
40/60 PET/PC	133 ± 2
20/80 PET/PC	137 ± 1†
PC	—

DSC scan rate is 10°C/min.
† Overlaps with glass transition of PC.

recrystallization rate experiences a maximum with blend composition at about 60 wt % PET. However, it is not clear whether the enhancement of cold crystallization rate in the high PET content blends as compared with the modified PET containing the blend additives is statistically significant. The increase in recrystallization temperature in the high PC content blends is certainly significant and indicative of a strong depression in recrystallization rate. This depression of recrystallization rate is most likely the result of reduced mobility of the constrained PET chains in the high PC content blends.

Isothermal Crystallization Rate of PET/PC Blends

The isothermal crystallization rate of PET in the blends is taken as the inverse of the crystallization half-time, which is the time at which one half of the crystallization exotherm area has evolved. The crystallization rate of PET and modified PET with blend additives is shown in Figure 4 as a function of crystallization temperature. Crystallization rate in both systems decreases with increasing crystallization temperature, reflecting the decrease in undercooling from the melt at higher crystallization temperatures. For this regime of crystallization conditions, crystallization rate is expected to increase with increasing undercooling.

As shown in Figure 4, the isothermal crystallization rate of PET is significantly enhanced by the addition of transesterification inhibitor and antioxidant at all crystallization temperatures. This increase in crystallization rate may be the result of heterogeneous nucleation by one or both of the additives. Indeed, crystallization in this regime is expected to be nucleation controlled. It is also possible that one or both of the additives may chemically

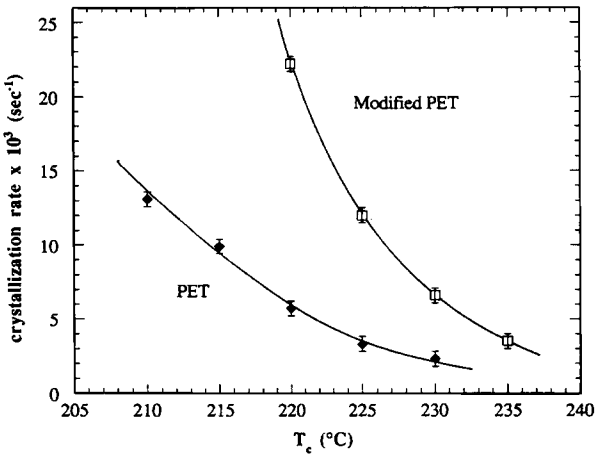

Figure 4 Crystallization rate of PET and modified PET with blend additives as a function of crystallization temperature.

react with PET, and that the mechanism of nucleation involves these reaction products. Alternatively, the addition of transesterification inhibitor and antioxidant may affect the linear growth rate of spherulites through an enhancement of molecular mobility.

Figure 5 shows the crystallization rate of PET/PC blends as a function of crystallization temperature. The crystallization rate of modified PET containing the same additives as the blends is given in order to provide a proper basis for comparison. The PC component has a significant effect on the crystallization rate of PET, and the magnitude of the effect depends on blend composition. The 60/40 PET/PC blend shows an enhancement of PET crystallization rate over that of 100% PET which is

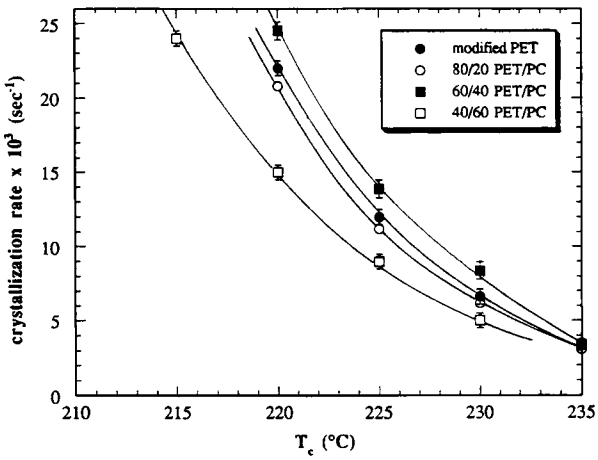

Figure 5 Crystallization rate of modified PET with blend additives and PET/PC blends as a function of crystallization temperature.

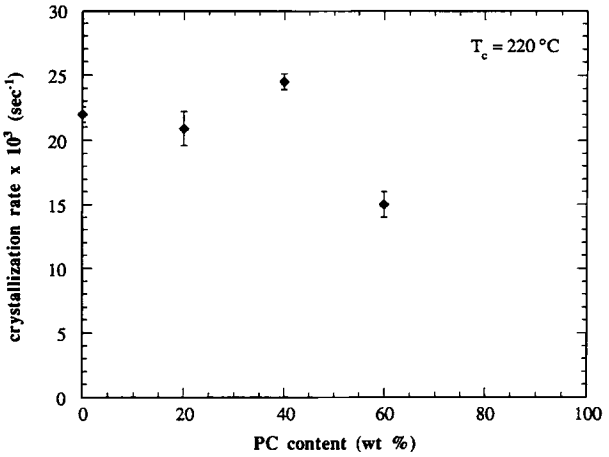

Figure 6 Crystallization rate of PET in PET/PC blends as a function of PC content in the blend.

most pronounced at the lower crystallization temperatures. The crystallization rate of PET in the 80/20 PET/PC is approximately equal to that of the PET with blend additives across the temperature range studied. The 40/60 PET/PC blend shows a significant depression of PET crystallization rate from that of the modified PET. It was not possible to observe isothermal crystallization exotherms for 20/80 PET/PC due to the weak signal, which could not be separated from the DSC machine response in quenching to the crystallization temperature.

Figure 6 shows the crystallization rate of PET at T_c of 220°C as a function of PC content. The rate passes through a maximum at a PC content of 40 wt % probably due to nucleation of crystallization at the interface between the PET and PC domains. This effect is likely to be small compared with the effect of the blend additives, as discussed earlier, since the additives are dispersed throughout the PET phase. This nucleation effect at the PET/PC interface is too small to be observed in the 80/20 PET/PC. Alternatively, PC chains in their rubbery state may enhance PET mobility at the interface between the phases, thereby affecting the rate of crystallization. Enhancement of linear growth rate of spherulites has been observed in poly(methyl methacrylate)/PET blends[6] and may be related to mobility effects.

As PC content increases, the rate-enhancing effect of PC appears to be overwhelmed by physical interference of PC domains with PET crystallization. The strong suppression of crystallization rate at high PC content may also reflect excessive dilution of the PET in the blend. Previous studies using infrared spectrophotometry have also concluded that blends with high PC content display a suppression or alteration of PET crystallinity; however, crystallization rates were not investigated.[5,17]

Degree of Crystallinity

The degree of crystallinity of PET achieved during isothermal crystallization is determined from the fusion scans following crystallization. The degree of crystallinity is the heat of crystallization (experimental heat of fusion) divided by the heat of crystallization of a theoretical 100% crystalline sample, which is taken to be 33 cal/g.[18] As shown in Table III, the degree of crystallinity of PET, modified PET with blend additives, and 60/40 PET/PC does not significantly depend on crystallization temperature. This agrees with a previous study of PET crystallization.[19]

Because degree of crystallinity is found not to depend on crystallization temperature in a systematic way, we have chosen to average the results for a given blend over the crystallization temperature range studied, and the data for all blend systems are summarized in Table IV. The value of degree of crystallinity for the 20/80 PET/PC blend was determined using the heat of fusion from the initial scan, since no isothermal crystallization exotherms were observed. The degree of crystallinity of PET in the high PC content blends is depressed as compared with 100% PET. Depression in degree of crystallinity has previously been reported for these blends.[5,14] Degree of crystallinity begins to drop off sharply as PC content in the blends approaches 80%. These results present an interesting complement to the crystallization rate results. Crystallization rate as a function of PC content begins to decrease sharply after 60 wt % PC content. Together, these results indicate that in high PC content blends the amorphous phase interferes with the development of crystallinity in the PET phase. Alternatively, it

Table III Degree of Crystallinity (%) of PET, PET with Blend Additives, and 60/40 PET/PC as a Function of Isothermal Crystallization Temperature

T_c (°C)	PET	Modified PET	60/40 PET/PC
215	33 ± 2		
220	34 ± 1	33 ± 1	33 ± 1
225	34 ± 1	34 ± 1	33 ± 2
230	36 ± 1	34 ± 1	33 ± 1
235	36 ± 1	34 ± 1	34 ± 1

Results are the average of three measurements, and error limits are the standard deviation.

Table IV Degree of Crystallinity of PET in Blend Samples as Determined from DSC Fusion Endotherms Following Crystallization

Sample	Degree of Crystallinity (%)
PET	35 ± 1
Modified PET	34 ± 1
80/20 PET/PC	32 ± 1
60/40 PET/PC	33 ± 1
40/60 PET/PC	30 ± 2
20/80 PET/PC	12 ± 2†
PC	0†

Values given are the mean of 12 measurements over four crystallization temperatures, and error limits are the standard deviation.

† From heat of fusion of quenched sample after scan from 25°C; value given is the mean of three measurements.

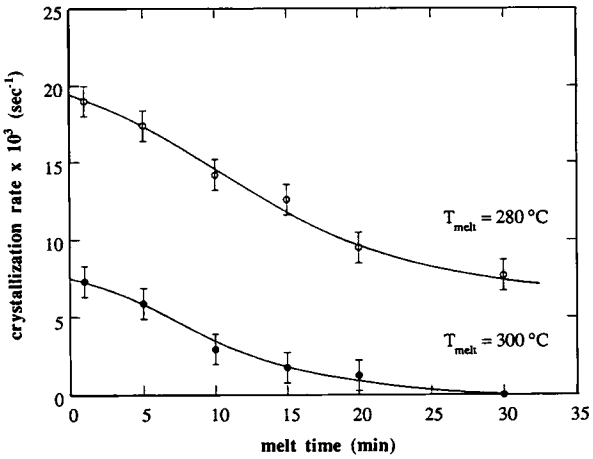

Figure 7 PET crystallization rate in 60/40 PET/PC as a function of melt processing time for melt processing temperatures of 280 and 300°C.

is possible that substantial transesterification occurred, which would impair the ability of the PET phase to crystallize.

Effect of Thermal Treatment on Crystallization

The effect of thermal treatment on the crystallization of PET/PC blends was examined for the case of 60/40 PET/PC. Thermal treatment effects are particularly interesting in this system due to the possibility of ester exchange reactions. The crystallization rate of 60/40 PET/PC as a function of the time held in the melt prior to crystallization is shown in Figure 7 for two different melt processing temperatures, 280°C and 300°C. Melt processing temperature is seen to have a much stronger effect on crystallization rate than melt hold time. All samples held at 300°C crystallize more slowly than those held at 280°C, regardless of the time they were held in the melt. However, there is some effect of melt hold time. For both melt temperatures, the longer the melt hold time, the slower the crystallization. There are two factors which may contribute to this depression in crystallization rate. Higher melt processing temperatures and longer processing times result in the destruction of more residual crystallites, which would reduce the density of nuclei, thus slowing subsequent crystallization. Also, longer melt times and higher temperatures may contribute to transesterification and other degradation reactions, which may slow crystallization.

Figure 8 shows the effect of thermal processing on degree of crystallinity. Again, melt temperature has a stronger effect on crystallinity than melt time. The marked depression in final degree of crystallinity in the samples held at 300°C seems to be strong evidence that transesterification or other degradation has occurred. If the effect of melt treatment were simply the destruction of residual crystallites, it is not likely that the ultimate crystalline perfection of the material in subsequent crystallizations would be affected. The observed depression is more likely the result of reactions occurring in the melt which prevent the material from crystallization. Degree of crystallinity in the samples held at 280°C prior to crystallization is unaffected for processing times up to 10 min. For melt processing times greater than 10 min, there appears to be a slight depression in degree of crystallinity; however, this effect is on the order of the uncertainty of the measurements.

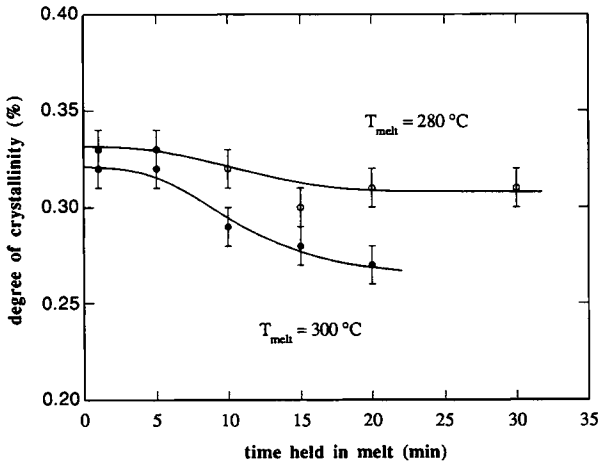

Figure 8 PET degree of crystallinity in 60/40 PET/PC as a function of melt processing time for melt processing temperatures of 280 and 300°C.

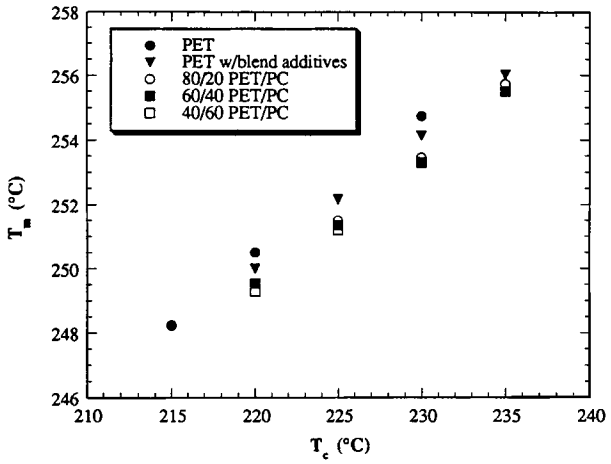

Figure 9 Melting temperature as a function of crystallization temperature for PET, modified PET with blend additives, and PET in PET/PC blends.

Melting Behavior

Figure 9 shows the melting temperature of PET and PET/PC blends as a function of crystallization temperature. As expected, the melting temperature increases with crystallization temperature, but the differences among the various systems are small. There is no significant effect of blend additives on T_m, and the small depression that is observed at most crystallization temperatures is within the uncertainty in the measurements. The absence of an effect of blend additives on T_m agrees with the results for degree of crystallinity.

There is a small effect of blending with PC on the melting temperature of PET. The small depression in T_m of PET in 80/20, 60/40, and 40/60 PET/PC as compared with PET is systematic and slightly greater than the uncertainty in the measurements. It is possible that the magnitude of the T_m effect is reduced as a result of annealing during the melting scan. Annealing would tend to obscure a depression in T_m, as annealed crystals melt at a higher temperature than crystals which have not undergone a perfecting process. The small depression in T_m is consistent with the depression in degree of crystallinity observed in the blend systems, particularly for high PC contents. The small reduction in perfection of the PET crystal phase in PET/PC may be the result of constrained growth due to the presence of amorphous PC domains. Alternately, it is possible that some transesterification has occurred, introducing PET/PC copolymer and thereby defects into crystals.

The equilibrium melting temperature, T_m°, of PET was determined by the method of Hoffman and Weeks[20] for the systems shown in Figure 9. The results are given in Table V. T_m° is significantly depressed in PET/PC blends and PET with blend additives as compared with PET, reflecting a less perfect crystal phase which is probably the result of the enhanced crystallization rate in these systems, as compared with that of unmodified PET.

While the experimental melting temperature of PET in PET/PC blends is slightly depressed as compared with modified PET with blend additives, as shown in Figure 9, the equilibrium melting temperature determined by the method of Hoffman and Weeks is not. Most probably, the differences in the equilibrium melt temperature that might have been expected on the basis of differences in T_m are not observed because of the narrow range of crystallization temperatures investigated, which causes considerable uncertainty in the extrapolation required in the Hoffman and Weeks method.

Dynamic Melt Crystallization

Dynamic melt crystallization of PET in PET/PC blends was examined in cooling scans, as shown in Figure 10. The step change in baseline seen at roughly 140°C is related to T_g of PC. T_g of PET is not observed, presumably because of masking by PET crystallinity developed earlier in the scan.

In PET and in high PET content blends, a crystallization exotherm is observed at approximately 220°C. In the 20/80 PET/PC scan, the PET crystallization exotherm is much smaller and shifted to lower temperatures. The smaller exotherm in the 20/80 PET/PC reflects the significantly reduced degree of crystallinity previously observed in this blend. The shift to lower temperature indicates a substantial depression in dynamic crystallization rate in this system as compared with the higher PET content blends. This agrees with the results of the isothermal crystallizations discussed earlier. Iso-

Table V Equilibrium Melting Temperature, T_m°, of PET in Blend Samples as Determined by the Method of Hoffman and Weeks

Sample	T_m° (°C)
PET	276 ± 2
Modified PET	270 ± 3
80/20 PET/PC	270 ± 2
60/40 PET/PC	269 ± 2
40/60 PET/PC	269 ± 2

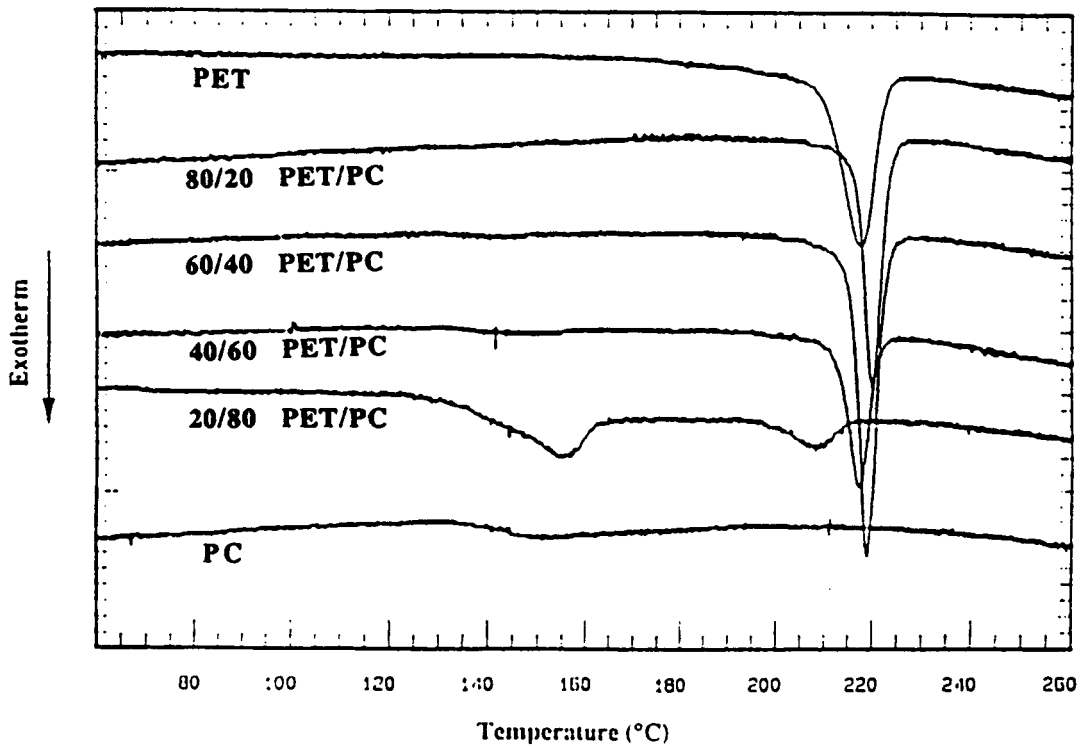

Figure 10 Cooling scans of PET/PC blends showing the dynamic melt crystallization of PET/PC.

thermal crystallization of 20/80 PET/PC was found to be very weak.

We also observed a second crystallization exotherm for the 20/80 blend at 155°C immediately above the T_g of PC. To verify this second exotherm, a sample of 10/90 PET/PC was produced by combining films of 100% PC and 20/80 PET/PC during the molding process. Similarly, a sample of 30/70 PET/PC was prepared by combining a 20/80 PET/PC film with a 40/60 PET/PC film. It was assumed that the molding process would provide adequate mixing to produce uniform blends of the intermediate compositions.

The dynamic scans for these materials are shown in Figure 11. It is interesting that the size of the low-temperature exotherm appears to increase with increasing PC content of the sample. Figure 12 shows the area of the low-temperature exotherm as a function of PC content in the blend. On a per gram PET basis, the heat evolved during the low-temperature process is 1.0 cal for the 70% PC blend, 1.8 cal for the 80% PC blend, and 2.5 cal for the 90% PC blend. In contrast, the high-temperature exotherm is larger in 30/70 PET/PC than in 20/80 PET/PC, and the peak maximum moves closer to that of the 40/60 PET/PC. The high-temperature exotherm is no longer distinguishable in the 10/90 PET/PC scan.

These results confirm that in PET/PC blends with PC contents greater than 60%, there are two PET crystallization exotherms observable in dynamic crystallization from the melt. The high-temperature exotherm, at roughly 210°C, appears to be related to normal PET crystallization. The second exotherm at 155°C may be related to PC or a cocrystalline form of PET and PC. It is also possible that the second exotherm results from the formation of a different crystal superstructure. Perhaps highly constrained growth occurring in high PC content blends takes the form of axialites or platelike growth.

MODELING THE CRYSTALLIZATION KINETICS

The Avrami Model

The Avrami model for the volume fraction crystallized as a function of time, $C(t)$, leads to the following equation:

$$1 - C(t) = e^{-Kt^n} \quad (1)$$

where K is the Avrami rate constant and n is the Avrami exponent. The Avrami model suggests the possibility of superposition of results obtained at different crystallization temperatures.[21] That is, if a system typically crystallizes in a given growth geometry and by a given nucleation mechanism, plots of crystalline fraction as a function of time at different temperatures may be superimposed on one another by using a shift factor involving crystallization half-time. When $t = t_{1/2}$, $C(t) = 0.5$ and the Avrami equation becomes

$$0.5 = \exp(-Kt_{1/2}^n) \tag{2}$$

From Eq. (2) the Avrami rate constant can be expressed in terms of $t_{1/2}$ and n:

$$K = \ln 2/t_{1/2}^n \tag{3}$$

By using Eq. (3) in Eq. (1), the Avrami equation may be written as

$$1 - C(t) = \exp[(-\ln 2)(t/t_{1/2})^n] \tag{4}$$

Thus, for systems which obey Avrami behavior and which have the same nucleation mechanism and growth morphology, $C(t)$ curves are expected to superimpose when plotted as a function of $t/t_{1/2}$.

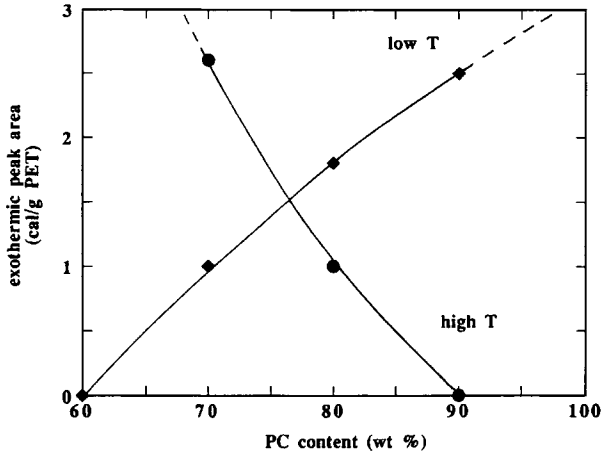

Figure 12 Heat of crystallization of the low- and high-temperature exotherms in dynamic melt crystallization of PET/PC as a function of PC content of the blend.

Figure 13 shows $C(t)$ as a function of $t/t_{1/2}$ for PET at five crystallization temperatures between 210°C and 230°C. Each point on this plot is the average of three measurements, and clearly the curves for various temperatures superimpose very well. This indicates that the crystallization of PET

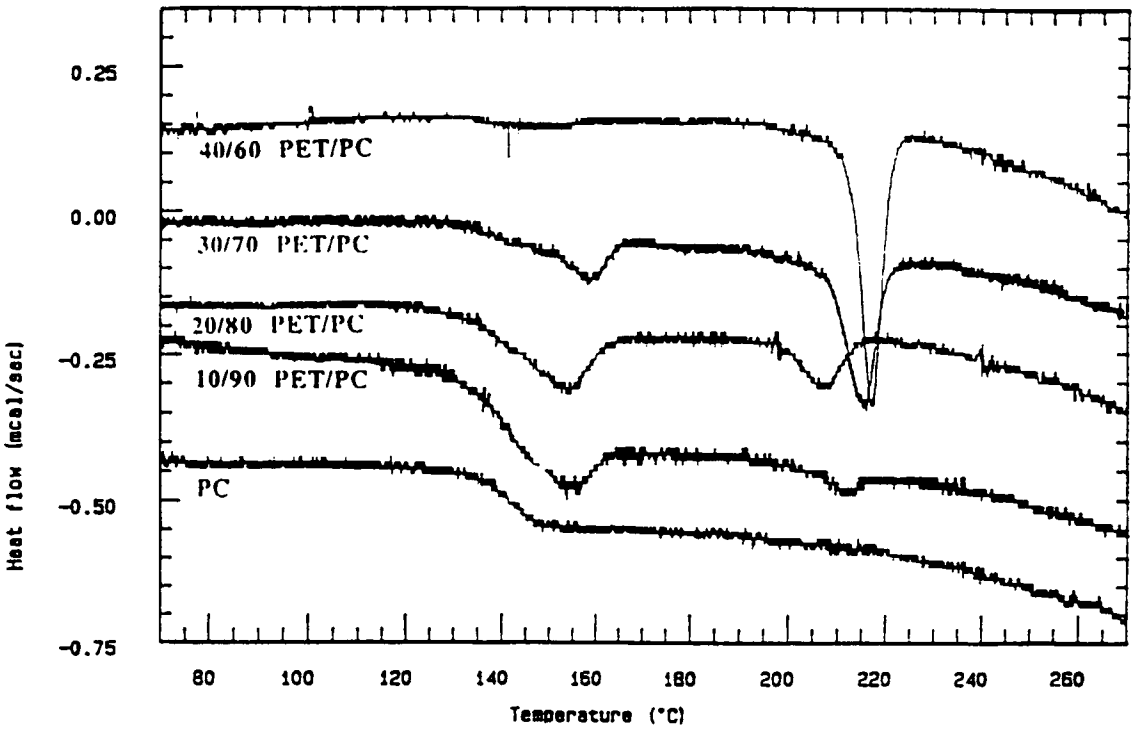

Figure 11 Cooling scans of PET/PC blends showing dual peak dynamic melt crystallization behavior of low PET content PET/PC blends.

at temperatures between 210°C and 230°C occurs by the same nucleation mechanism and growth morphology. It seems that the difference in crystallization at various temperatures is marked by differences in nucleation and growth rates, not by variation in crystallization mechanism.

The solid line in Figure 13 is the Avrami equation for $n = 2$. Comparing experimental results with the Avrami equation indicates that the Avrami model predicts the development of crystallinity very well during the initial stages of crystallization. However, in the later stages of growth, the experimental results show that PET crystallinity does not develop as rapidly as the Avrami model predicts. This slowing may reflect a depression in linear growth rate of spherulites in the later stages of growth, or perhaps growth becoming more constrained. Both of these possibilities are consistent with secondary crystallization following primary spherulitic crystal growth.

Figure 14 shows the superposition plot of relative crystallinity as a function of $t/t_{1/2}$ for modified PET containing blend additives. Again, the curves at different crystallization temperatures superimpose, indicating a similar crystallization mechanism at all temperatures. The best-fit Avrami equation to the early portion of the crystallinity curve has an Avrami exponent of 2.75. This is substantially higher than that for PET without blend additives. The usual interpretation of an increase in Avrami exponent is a shift from athermal nucleation to thermal nucleation, for the same growth morphology. Alternatively, a higher Avrami exponent may reflect a transition to less constrained growth, such as a transition from two-dimensional to three-dimensional growth. We have previously suggested that one or both of the blend additives acts as a nucleating agent for PET crystallization, which is not inconsistent with the athermal/thermal shift mechanism.

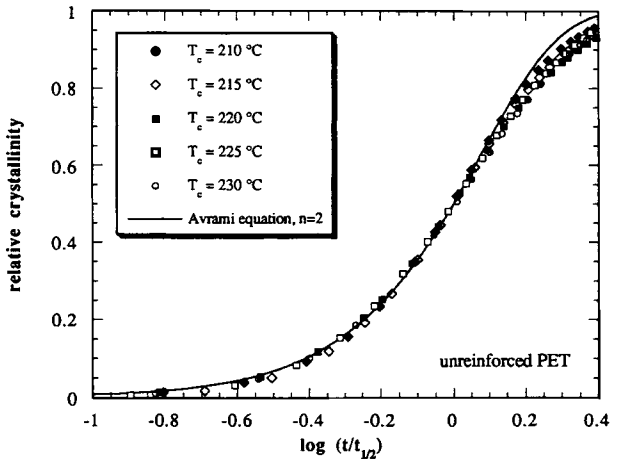

Figure 13 Plots of relative crystallinity as a function of $t/t_{1/2}$ for PET showing the superposition of data collected at different temperatures.

In modified PET, as in PET, there is significant deviation from the Avrami equation in the later stages of growth. The departure from the Avrami prediction is more significant in modified PET with blend additives than in PET. This departure, as discussed earlier, may be the result of secondary crystallization processes, which would be expected to be particularly important in the faster crystallizing modified PET. More rapidly formed crystallites may be expected to undergo greater secondary crystallization because of imperfections and trapped amorphous regions formed during rapid initial crystallization.

Figures 15 and 16 show the superposition of relative crystallinity curves for 80/20 PET/PC and 60/40 PET/PC, respectively. The Avrami equation, which provides a good fit to the initial portion of these curves, has an exponent of 3.0 for both blends. This is slightly higher than that for modified PET (the same PET as in the blends). Again, this increase in n is interesting, as a possible interpretation for increasing Avrami exponent is less constrained growth. One would not expect growth to be less constrained in blends as compared with modified PET. If anything, the amorphous PC domains would be expected to produce more constrained PET crystalline domains. The blend systems also display a substantial departure from the Avrami prediction for crystallinity in the later stages of crystallization.

The Series Avrami Model

In the preceding discussion, it was postulated that departure from the Avrami model prediction in the later stages of growth is the result of secondary crystallization. If this is the case, a model which accounts for two crystallization processes would seem to be appropriate for modeling the PET crystallization kinetics. Velisaris and Seferis[22] have proposed a model based on two processes occurring in series, each of which obeys Avrami behavior. The development of crystallinity over time is described by

$$1/C(t) = w_1/(1 - \exp(-K_1 t^{n_1})) + (1 - w_1)/(1 - \exp(-K_2 t^{n_2}) \quad (5)$$

where w_1 is the weight factor for the first process, K_1 and n_1 are the Avrami rate constant and exponent for the first process, $(1 - w_1)$ is the weight factor for

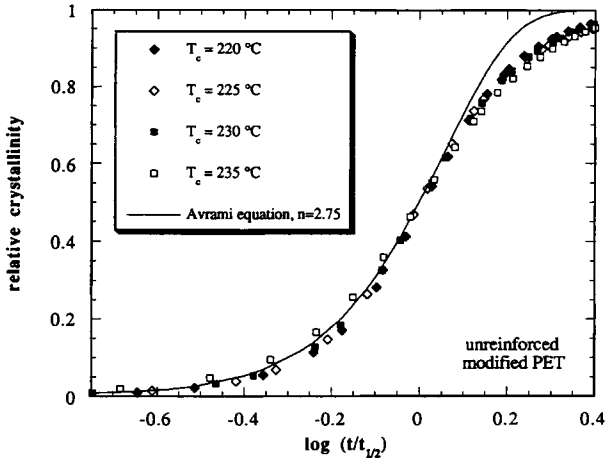

Figure 14 Plots of relative crystallinity as a function of $t/t_{1/2}$ for modified PET with blend additives showing the superposition of data collected at different temperatures.

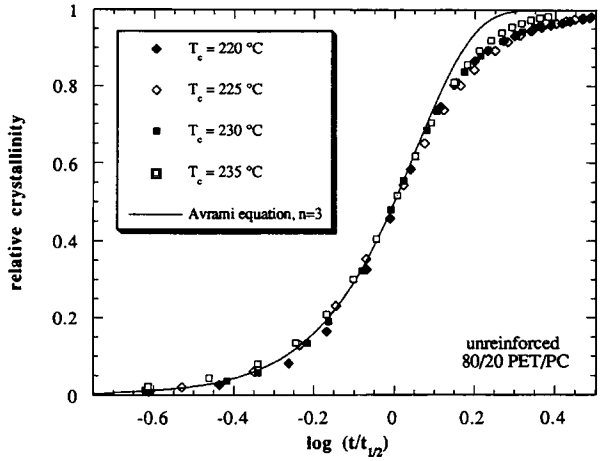

Figure 15 Plots of relative crystallinity as a function of $t/t_{1/2}$ for 80/20 PET/PC blend showing the superposition of data collected at different temperatures.

the second process, and K_2 and n_2 are the Avrami rate constant and exponent for the second process.

Since we have shown from superposition that for a given system the nucleation mechanism and growth morphology are similar for all temperatures, the series Avrami model may be modified as follows: Rather than optimizing n_1, n_2, w_1, K_1, and K_2 at each crystallization temperature, average n_1 and n_2 for the crystallization temperature range are used and only w_1, K_1, and K_2 are optimized. By modeling the crystallization kinetics using this three-parameter series model, the units of K_i ($i = 1$ or 2) are the same for all crystallization temperatures, allowing K_i to be compared for all crystallization temperatures for a given system. In contrast, when n_1 and n_2 are optimized in the five-parameter series Avrami model, the units of K_i are min^{-n_i} and are likely to vary somewhat with crystallization temperature. Constant units of K_i are an important advantage of using the modified three-parameter series Avrami model.

The average Avrami exponent for a given system is determined by first solving the five parameter series model [Eq. (5)]. All possible Avrami exponent solutions for a given crystallization temperature are averaged using the percent error of the fit as a weighting factor. The average Avrami exponent for the first process, $\bar{n}_1$, is then determined as the average of the weighted averages for each crystallization temperature. The average Avrami exponent for the second process, $\bar{n}_2$, is determined in the same way. The series Avrami model is then fit to the $C(t)$ data using the average Avrami exponents. This three-parameter series model takes the form

$$1/C(t) = w_1/(1 - \exp(-\bar{K}_1 t^{\bar{n}_1})) + (1 - w_1)/(1 - \exp(-\bar{K}_2 t^{\bar{n}_2}) \quad (6)$$

where $\bar{K}_1$ and $\bar{K}_2$ are the Avrami rate constants for the first and second processes, based on the average Avrami exponents. The units of $\bar{K}_1$ are $\text{min}^{-\bar{n}_1}$, and the units of $\bar{K}_2$ are $\text{min}^{-\bar{n}_2}$.

A FORTRAN 77 program was created to fit Eq. (6) to the experimental data using a Levenberg–Marquardt optimization routine.[23] The $C(t)$ results of three runs performed on different specimens were first averaged for each crystallization temperature and polymer system considered. The averaged $C(t)$ data were fit with Eq. (6). Figure 17 shows a sample plot of data of relative crystallinity as a function of

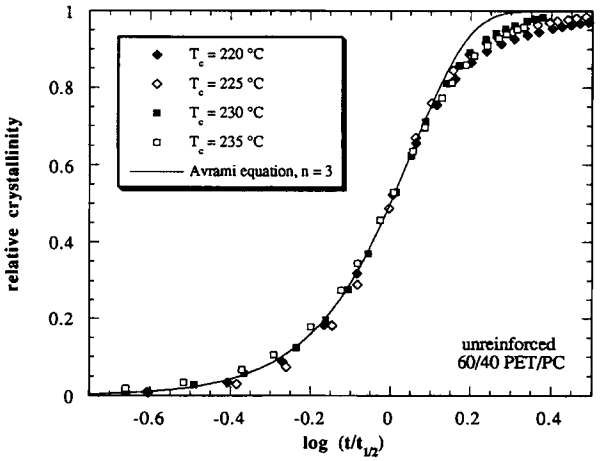

Figure 16 Plots of relative crystallinity as a function of $t/t_{1/2}$ for 60/40 PET/PC blend showing the superposition of data collected at different temperatures.

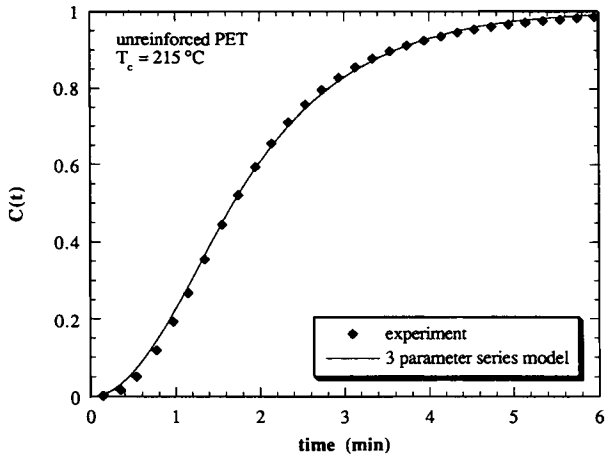

Figure 17 Comparison of results for three-parameter series Avrami model and experimental crystallization of PET at 215°C.

time for PET and the best-fit line to the data using the three-parameter series Avrami model. Clearly, the three-parameter series Avrami model is successful in describing the crystallization of PET during all stages of the crystallization process. We do note, however, that the error in applying the three-parameter model is typically larger than that for the five-parameter series Avrami model. This is the expected outcome of optimizing three parameters rather than five.

The results for w_1, $\bar{n}_1$, $\bar{K}_1$, $\bar{n}_2$, and $\bar{K}_2$ for each of the systems studied are given in Tables VI and VII for crystallization temperatures of 220°C and 230°C, respectively. As would be expected from the preceding discussion, $\bar{n}_1$ is larger for modified PET and PET/PC than for PET. The value of $\bar{n}_2$ is between 1.5 and 2.0 for all systems, which may reflect a combination of one-dimensional and two-dimensional athermally nucleated growth. Such an interpretation is also consistent with secondary crystallization. As would be expected, blend additives and blending have little effect on the Avrami exponent of a secondary process.

The trends in $\bar{K}_1$ follow those in crystallization half-time: Modified PET with blend additives, 80/20 PET/PC, and 60/40 PET/PC have $\bar{K}_1$ values significantly higher than PET. This correlation is expected as both crystallization half-time and $\bar{K}_1$ reflect the early stages of crystallization. It is interesting that $\bar{K}_2$ is also greater for modified PET and PET/PC than for PET. It is possible that there are more growth events associated with the secondary process in modified PET and PET/PC. The greater frequency of these events would contribute to larger $\bar{K}_2$ values. However, there is no trend in w_1 values which corresponds with this suggestion.

The temperature-dependent behavior of the three-parameter series Avrami model rate constants were examined assuming an Arrhenius-type temperature dependence. The rate constant of the ith process is assumed to depend on crystallization temperature according to

$$K_i = A_i \exp(-E_{a,i}/R\Delta T) \tag{7}$$

where $i = 1$ or 2, A_i is the Arrhenius frequency factor for the ith process, $E_{a,i}$ is the activation energy for the ith process, R is the ideal gas constant, and ΔT is the undercooling from the melt or $T_m^\circ - T_c$. A_1, $E_{a,1}$, A_2, and $E_{a,2}$ are given in Table VIII for all systems considered.

For all systems, the frequency factor for the first process is greater than that of the second process. This indicates that, for a given system, there are more crystal growth events associated with the first process than the second, which is consistent with the suggestion that there is primary growth followed by secondary crystallization. It seems reasonable that the primary development of crystallinity would be associated with more crystallization events than the secondary processes involving crystal perfection.

Table VI Three-Parameter Series Avrami Model Best-Fit Parameters for Isothermal Crystallization at 220°C of PET and PET/PC

Matrix	Reinforcing Fiber	w_1	$\bar{K}_1$ (min^{-n_1})	$\bar{n}_1$	$\bar{K}_2$ (min^{-n_2})	$\bar{n}_2$	Error (%)
PET	Neat	0.73	0.04	2.39	0.05	1.76	8.54
Modified PET	Neat	0.82	2.26	3.37	0.52	1.96	0.37
80/20 PET/PC	Neat	0.88	1.52	3.22	0.42	1.64	0.96
60/40 PET/PC	Neat	0.90	3.51	3.71	0.44	1.61	0.47

The average value of the first and second Avrami exponent used for the model are also provided.

Table VII Three-Parameter Series Avrami Model Best-Fit Parameters for Isothermal Crystallization at 230°C of PET and PET/PC Composites

Matrix	Reinforcing Fiber	w_1	$\bar{K}_1$ ($\min^{-n_1}$)	$\bar{n}_1$	$\bar{K}_2$ ($\min^{-n_2}$)	$\bar{n}_2$	Error (%)
PET	Neat	0.55	0.02	2.39	0.01	1.76	0.38
Modified PET	Neat	0.80	0.05	3.37	0.04	1.96	0.68
80/20 PET/PC	Neat	0.59	0.11	3.22	0.11	1.64	8.50
60/40 PET/PC	Neat	0.75	0.10	3.71	0.09	1.61	6.00

The average value of the first and second Avrami exponent used for the model are also provided.

The Arrhenius results in Table VIII indicate that the activation energy of the first process is greater than that of the second process for all systems. This result seems consistent with the conclusion that the second series process is secondary crystallization. The lower activation energy of the second process may be interpreted to indicate that the second process is dominated by the perfection of existing crystalline regions.

The effect of blend additives on the frequency factor of the first crystallization process is significant. The frequency factor of modified PET is approximately four times that of unreinforced PET, which would confirm that one or both of the blend additives can nucleate PET. However, the Arrhenius results suggest that nucleation may not be the only means by which these blend additives affect the crystallization of PET. The activation energy of the first process is depressed in modified PET as compared with PET. This result suggests that blend additives may affect the nature of the crystallization process, such that the energy barrier to crystallization is reduced (e.g., by having a plasticizing effect or by reducing molecular weight).

Blend additives also produce an enhancement of the frequency factor of the second series process. As discussed in the case of fiber-reinforced PET, this may be the result of the enhancement of crystallization rate in modified PET. Increased crystallization rate may result in less perfect crystals and more material available for secondary crystallization. It is possible that there is an effect on activation energy as well, but the depression of $E_{a,2}$ in modified PET is slight.

The activation energy for the first and second processes is also significantly depressed in 80/20 PET/PC and 60/40 PET/PC as compared with PET. These results are similar to those for modified PET and may therefore reflect the effect of blend additives. It is also interesting that the frequency factor for the second process is substantially depressed as compared with PET and modified PET. This depression may be due to the presence of the amorphous PC phase. As discussed earlier, the degree of crystallinity of PET is slightly lower in the blends, which may be related to less vigorous secondary crystallization.

CONCLUSIONS

An increase in T_g of PET and decrease in T_g of PC in blended samples over pure polymer have been observed. These shifts may be the result of glass–rubber interactions or transesterification. For blends containing more than 20 wt % PET, there is an enhancement of isothermal PET crystallization rate from the melt. A depression in degree of crystallinity of PET is observed in blended PET as compared with pure PET, particularly for high PC content

Table VIII Arrhenius Frequency Factor and Activation Energy of the First and Second Process Avrami Rate Constant for the Series Avrami Model

Matrix	A_1 ($\times 10^3$ $\min^{-n_1}$)	$E_{a,1}$ (kcal/mol)	A_2 ($\times 10^3$ $\min^{-n_2}$)	$E_{a,2}$ (kcal/mol)
PET	62.1	1.54	2.83	1.19
Modified PET	236	1.17	4.13	0.90
80/20 PET/PC	14.2	0.94	1.23	0.77
60/40 PET/PC	718	1.23	0.20	0.59

blends. These results reflect a less perfect final crystalline form of PET in the blends, which may be the result of transesterification or simply an interference of the amorphous PC phase with the development of crystallinity. Strong effects of thermal history on blend crystallization kinetics were observed, particularly for higher melt temperatures. In dynamic crystallization experiments from the melt, for PET/PC blends containing between 10% and 30% PET in the blend, two crystallization exotherms at approximately 210°C and 155°C are observed. The high-temperature exotherm appears to be related to normal PET crystallization. However, the lower temperature exotherm (just above T_g of PC) increases in magnitude with PC content and may reflect a co-crystalline form of PET and PC.

The Avrami model was applied to the crystallization kinetics of PET, modified PET, and PET/PC blends. As predicted from the form of the Avrami equation, relative crystallinity plots obtained at different crystallization temperatures superimpose when plotted as a function of $t/t_{1/2}$. However, the Avrami model failed to describe the kinetics in the later stages of crystallization. In order to describe all stages of crystallization, a weighted series Avrami model was employed, which successfully described the entire crystallization process in terms of primary crystallization followed by slow, constrained secondary crystallization.

The authors thank Dr. William Richards and the General Electric Company for providing the blends used in this study. They also thank Taconic Plastics for providing the mold release fabrics used. They gratefully acknowledge the optical microscopy work of Mrs. Sigrid Ruetsch of TRI/Princeton.

REFERENCES

1. T. R. Nassar, D. R. Paul, and J. W. Barlow, *J. Appl. Polym. Sci.*, **23,** 85 (1979).
2. T. Suzuki, H. Tanaka, and T. Nishi, *Polymer,* **30,** 1287 (1989).
3. Z. H. Huang and L. H. Wang, *Makromol. Chem., Rapid Commun.*, **7,** 255 (1986).
4. Q. Tan and D. Z. Ma, *J. Appl. Polym. Sci.*, **48,** 747 (1993).
5. X.-Y. Chen and A. W. Birley, *British Polym. J.*, **17,** 347 (1985).
6. K. Kugo, T. Kitaura, A. Kodera, J. Nishino, and N. Ikuta, *Sen-i Gakkaishi,* **49,** 98 (1993).
7. W. N. Kim and C. M. Burns, *J. Polym. Sci., Polym. Phys.*, **28,** 1409 (1990).
8. R. S. Porter, J. M. Jonza, M. Kimura, C. R. Desper, and E. R. George, *Polym. Eng. Sci.*, **29,** 55 (1989).
9. F. Pilati, E. Marianucci, and C. Berti, *J. Appl. Polym. Sci.*, **30,** 1267 (1985).
10. K. P. McAlea, J. M. Schultz, K. H. Gardner, and G. D. Wignall, *Polymer,* **27,** 1581 (1986).
11. M. Dröscher, *Ind. Eng. Chem. Prod. Res. Dev.*, **21,** 126 (1982).
12. W. G. Zheng, Z. H. Wan, Z. N. Qi, and F. S. Wang, *Polymer,* **34,** 4982 (1993).
13. A. Golovoy, M.-F. Cheung, K. R. Carduner, and M. J. Rokosz, *Polym. Eng. Sci.*, **29,** 1226 (1989).
14. S. R. Murff, J. W. Barlow, and D. R. Paul, *J. Appl. Polym. Sci.*, **29,** 3231 (1984).
15. B. D. Hanrahan, S. R. Angeli, and J. Runt, *Polym. Bull.*, **15,** 455 (1986).
16. L. C. Sawyer and D. T. Grubbs, *Polymer Microscopy,* Chapman Hall, London (1987).
17. A. W. Birley and X.-Y. Chen, *British Polym. J.*, **16,** 77 (1984).
18. A. Mehta, U. Gaur, and B. Wunderlich, *J. Polym. Sci., Polym. Phys. Ed.*, **16,** 289 (1978).
19. V. E. Reinsch and L. Rebenfeld, *J. Appl. Polym. Sci.*, **52,** 649 (1994).
20. J. D. Hoffman and J. J. Weeks, *J. Chem. Phys.*, **37,** 1723 (1962).
21. K. Ravindranath and J. P. Jog, *J. Appl. Polym. Sci.*, **49,** 1395 (1993).
22. C. N. Velisaris and J. C. Seferis, *Polym. Eng. Sci.*, **26,** 1574 (1986).
23. *Numerical Recipes in FORTRAN,* W. H. Press, S. A. Teukolsky, B. P. Flannery, and W. T. Vetterling, eds., Cambridge University Press, Cambridge, UK (1992).

Received May 8, 1995
Accepted May 29, 1995